Letters

Universal Control Scheme of Dual Three-Phase PMSM Drives With Single Open-Phase Fault

Kailiang Yu, *Student Member, IEEE*, Zheng Wang, *Senior Member, IEEE*, Minrui Gu, and Xueqing Wang

***Abstract*—The fault-tolerant control method of dual three-phase permanent-magnet synchronous motor (PMSM) drives has gained more and more attention in some applications, such as aircraft system and offshore wind energy system. In this letter, the reason for the torque ripple caused by the standard control method has been investigated in view of the frequency domain after the occurrence of a single open-phase fault. Based on the theoretical analysis, a universal control scheme has been proposed for the dual three-phase PMSM drives with two isolated neutral points, which can be implemented under either healthy condition or fault condition. The key is to modify with a closed-loop controller on harmonic subspace with the notch filter. The proposed method not only realizes the seamless transition between two operation conditions without fault diagnosis but also avoids the reconfiguration of the control structure. Moreover, the system optimization of the minimum copper loss under postfault condition has been integrated into the proposed method. The experimental results are presented to illustrate the effectiveness of the proposed method.**

***Index Terms*—Dual three-phase permanent-magnet synchronous motor (PMSM), minimum copper loss, single open-phase fault, universal control scheme.**

I. Introduction

MULTIPHASE motors have been intensively investigated in the past decades because of their inherent advantages, such as less current stresses per phase, reduced low-order torque ripples, and high fault-tolerant ability [1]. Among these merits, the fault-tolerant ability is mandatory in some applications with strict requirements for safety, such as electric vehicles or aircraft system. Besides, it becomes more and more popular with the offshore wind energy system, where the immediate maintenance might not be available after fault occurrence [2].

Most of the pieces of literature published so far utilize fault localization and control reconfiguration to achieve a satisfactory postfault performance on single-phase open circuit [3]–[7]. Therefore, the primary thing of fault-tolerant control is diagnosis, and the fault information can be used for the transition from prefault control method to postfault control one. In general, the fault detection can be implemented in the model- and signal-based perspectives [4]. Yet, the time delay of fault localization makes the transition not smooth after the occurrence of the open-phase fault.

When the open-phase fault occurred in multiphase drives, the current constraint of the open-circuit condition results in the coupling relationship between different subspaces, which are independent in the healthy situation according to the vector space decomposition (VSD) theory [8]. To ensure the torque-ripple-free performance, the current reference in other subspaces (typically termed harmonic subspace in the literature [8]) should be modified from zero to some combination coefficients of torque current under the postfault control method [5]. These coefficients are specially designed by different optimized strategies, such as the minimum-loss (ML) strategy, the maximum torque (MT) strategy, and the full-range ML strategy [6]. With the appearance of ac components in current reference, the previous control structure of proportional–integer (PI) should be switched to proportional–resonant (PR) controllers or deadbeat predictive current control to guarantee the tracking performance [7]. However, the traditional perspective leads to the split of method design between the prefault situation and postfault one. Meanwhile, these aforementioned control methods rely on the fault location information and system modification in current reference, control configuration, and system model.

To avoid the diagnosis process of open-phase fault, the natural fault tolerance or self-healing capability of dual three-phase motor drives have been reported in [9] and [10]. As stated in [9], the main cause of performance failure of prefault standard control method is the conflict goal between the closed-loop current control of torque subspace (CCTS) and closed-loop current control of harmonic subspace (CCHS) under the fault situation. It is suggested in [9] that the natural fault-tolerance accompanied by an efficient prefault control can be achieved with disabling the CCHS by setting a low harmonic voltage saturation threshold. Different from [9], the CCHS has remained while the actual harmonic currents are used as the reference values iteratively [10]. Since the actual harmonic current can be considered as the balanced result of the closed-loop controllers on the torque subspace and the harmonic subspace, the iterative replacement

Manuscript received 5 June 2022; revised 7 July 2022; accepted 18 July 2022. Date of publication 1 August 2022; date of current version 6 September 2022. This work was supported in part by the National Natural Science Foundation of China under Grant 52077034 and in part by the Aeronautical Science Foundation of China under Grant 20200019069001. *(Corresponding author: Zheng Wang.)*

Kailiang Yu, Zheng Wang, and Minrui Gu are with the School of Electrical Engineering, Southeast University, Nanjing 211189, China (e-mail: kailiang_yu@seu.edu.cn; zwang@eee.hku.hk; 230228726@seu.edu.cn).

Xueqing Wang is with the College of Electrical Engineering, Sichuan University, Chengdu 610065, China (e-mail: wangxueqing231@163.com).

Color versions of one or more figures in this article are available at https://doi.org/10.1109/TPEL.2022.3195526.

Digital Object Identifier 10.1109/TPEL.2022.3195526

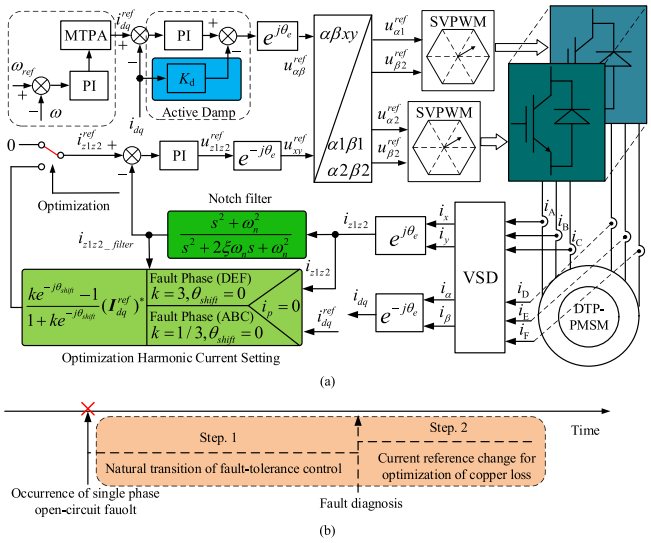

Fig. 1. (a) Proposed universal control scheme for dual three-phase PMSM drive with single-phase open-circuit fault. (b) Flowchart of the proposed method under fault situation.

of the actual harmonic current would enhance the CCTS and weaken the CCHS finally, which can reach the same results by disabling the CCHS in [9]. Although the smooth transition can be obtained in the methods above without use of fault diagnosis; some optimization targets for postfault condition, such as ML and MT, are difficult and even impossible to be integrated. Moreover, the enhanced phase-locked loop in [10] increases the complexity of the fault-tolerant structure.

In this letter, a universal control scheme has been proposed for the single open-phase fault of dual three-phase permanent-magnet synchronous motor (PMSM) drives with two isolated neutral points. On the basis of [9], the reason of incompatible control goal between CCTS and CCHS has been further investigated in the frequency domain. Thanking to the notch filter with a specially designed cutoff frequency, the natural fault tolerance of the proposed method can be achieved by automatic separation of the unwanted negative-sequence components without the need for fault diagnosis. Furthermore, the minimum copper loss under postfault condition is derived by setting the positive-sequence components of harmonic current simply. Different from the perception of "diagnosis first and then tolerance" in the conventional fault-tolerant control schemes, the proposed universal control scheme can achieve the automatic fault tolerance having the torque-ripple-free performance without the need for fault diagnosis. The experiments have been carried out to validate the proposed method.

II. Proposed Universal Fault-Tolerant Control

A. Proposed Universal Control Scheme

Fig. 1 presents the proposed universal control scheme of the dual three-phase PMSM drive. Compared with the conventional one, three modules have been inserted into the proposed method. First, the notch filters, the cutoff frequency of which is twice the fundamental frequency, have been inserted into the feedback path of harmonic current. Second, the optimizing harmonic-current setting can provide the current reference to the closed-loop control of harmonic current under either normal operation or fault-tolerant condition. Third, the active damping has been integrated into the closed-loop current controller on torque subspace for improving its disturbance rejection ability against harmonic-current components. The inserted modules have been depicted with some colors, as shown in Fig. 1, from which it can be found that the proposed universal control scheme has small changes to the conventional one. It should be noted that the PI controller of the harmonic subspace employed in this letter can be replaced by the harmonic controller, such as PR controller, for suppressing current harmonics in $z1z2$ frame.

As shown in Fig. 1(b), the flowchart of the proposed method under faulty situation can be divided into two steps. After the natural fault-tolerance operation is automatically achieved by the proposed control method in Step 1, the harmonic-current references can be changed according to the fault detection in Step 2 for the minimum copper loss. The fault information can be detected by fault diagnosis methods, such as the evaluation of the current amplitude of each phase. In detail, the amplitude ratio is set as 3 when the fault position is located in the second set of three-phase winding, and the ratio is one-third for the fault in the first set of three-phase winding.

B. Negative-Sequence Current Components

Based on the VSD in [8], the dynamic model of the dual three-phase PMSM drive in synchronous reference frame can be expressed by

$$\begin{aligned} u_d &= R_s i_d + L_D \cdot di_d/dt - \omega L_Q i_q \\ u_q &= R_s i_q + L_Q \cdot di_q/dt + \omega\left(L_D i_d + \psi_m\right) \\ u_{z1} &= R_s i_{z1} + L_{\sigma s} \cdot di_{z1}/dt + \omega L_{\sigma s} i_{z2} \\ u_{z2} &= R_s i_{z2} + L_{\sigma s} \cdot di_{z2}/dt - \omega L_{\sigma s} i_{z1} \end{aligned} \tag{1}$$

where the subscripts dq and $z1z2$ stand for the variables in torque subspace and harmonic subspace, respectively.

On the other hand, the double-dq synchronous frames model, where each set of the three-phase stator windings can be treated as a basic unit, is also an effective way in the analysis. The relationship of a variable $\boldsymbol{F}$ between VSD model and double dq model can be illustrated by [11]

$$\begin{aligned} \boldsymbol{F}_{dq} &= 0.5(\boldsymbol{F}_{d1q1} + \boldsymbol{F}_{d2q2}) \\ \boldsymbol{F}_{z1z2} &= 0.5(\boldsymbol{F}_{d1q1} - \boldsymbol{F}_{d2q2})^* \end{aligned} \tag{2}$$

where the vector $\boldsymbol{F}$ represents for the voltage and current variables. The superscript "$*$" stands for the complex conjugate of variable. The subscripts 1 and 2 present the first set of three-phase windings and the second one, respectively.

It is assumed that the fault position of the open circuit is localized into the F-phase of the second set of three-phase windings. Owing to the isolated neutral points between two sets of three-phase windings, the phase currents in the faulty winding are satisfied and the relationship is given by

$$i_D + i_E = 0, \quad i_F = 0. \tag{3}$$

The fundamental of the steady-state current in phase D and phase E of (3) can be rewritten in current phasor as follows:

$$\dot{I}_D = I_{\text{fault}} e^{j\theta_0}, \quad \dot{I}_E = I_{\text{fault}} e^{j(\theta_0+\pi)}, \quad \dot{I}_F = 0 \tag{4}$$

where θ_0 is the initial angle of current phasor.

According to the methods of symmetric component in [12], the unbalanced three-phase quantities can be split up into its positive-sequence, negative-sequence, and zero-sequence components. Thus, the positive-sequence and the negative-sequence components of current phasors can be derived from (4) as follows:

$$\begin{aligned} \dot{I}_{D+} &= \left(\dot{I}_D + a\dot{I}_E + a^2\dot{I}_F\right)/3 = I\left(e^{j\theta_0} - ae^{j\theta_0}\right)/3 \triangleq I_p e^{j\theta_p} \\ \dot{I}_{D-} &= \left(\dot{I}_D + a^2\dot{I}_E + a\dot{I}_F\right)/3 = I\left(e^{j\theta_0} - a^2 e^{j\theta_0}\right)/3 \triangleq I_n e^{j\theta_n} \end{aligned} \tag{5}$$

where $a = e^{j2\pi/3}$. I_p and θ_p are the amplitude and the phase angle of positive-sequence current phasor, respectively. I_n and θ_n are the amplitude and the phase angle of negative-sequence current phasor, respectively.

From (5), the current vector of the fault windings containing the positive-sequence and the negative-sequence components in stationary reference frame can be expressed as follows:

$$\boldsymbol{I}_{\alpha\beta 2} = \underbrace{I_{p2} e^{j(\omega_e t + \theta_{p2})}}_{\text{positive-sequence}} + \underbrace{I_{n2} e^{j(-\omega_e t - \theta_{n2})}}_{\text{negative-sequence}}. \tag{6}$$

Applying the Park transformation, the current vector of (6) can be updated in synchronous rotating reference frame as follows:

$$\boldsymbol{I}_{d2q2} = \underbrace{I_{p2} e^{j\theta_{p2}}}_{\text{DC}} + \underbrace{I_{n2} e^{j(-2\omega_e t - \theta_{n2})}}_{\text{AC}}. \tag{7}$$

It should be pointed out that there exists ac components twice of the fundamental frequency under the open-circuit faults compared, while there are only the dc components in normal operation.

C. Incompatible Control Goal Between CCHS and CCTS

Since the motor torque is only determined by the currents in torque subspace, the torque-ripple free can be achieved even under the open-circuit faults as long as the current components of torque subspace in (2) are maintained as the dc form.

Compared with (7), it can be inferred that the current of the healthy windings must contain the ac components twice of the fundamental frequency, the phase of which is just opposite to that of fault windings, as given by

$$\boldsymbol{I}_{d1q1} = I_{p1} e^{j\theta_{p1}} + I_{n2} e^{j(-2\omega_e t - \theta_{n2} + \pi)}. \tag{8}$$

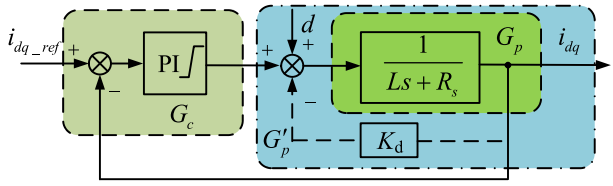

Fig. 2. Block diagram of CCTS with active damping under fault condition.

Substituting (7) and (8) into (2), the constant value of current component on torque subspace can be realized, as illustrated in the following equation (9) shown at the bottom of this page.

On the other hand, the current in harmonic subspace can be derived as follows:

$$\begin{aligned} \boldsymbol{I}_{z1z2} &= 0.5(I_{d1q1} - I_{d2q2})^* \\ &= \underbrace{0.5\left(I_{p1} e^{-j\theta_{p1}} - I_{p2} e^{-j\theta_{p2}}\right)}_{\text{DC}} - \underbrace{I_{n2} e^{j(2\omega t + \theta_{n2})}}_{\text{AC}}. \end{aligned} \tag{10}$$

It should be noted that the presence of ac current components on harmonic subspace makes it impossible to realize the traditional control objective on harmonic space, where the reference of harmonic current is set to zero under normal operation control. In other words, the negative-sequence components caused by the open-circuit faults make the control objectives of CCTS and CCHS incompatible. In order to guarantee the feasibility of torque-ripple free in torque subspace, the positive-sequence components instead of all components should be controlled in harmonic subspace under fault-tolerant condition. Therefore, the notch filters with the cutoff frequency twice of the fundamental one are inserted into the feedback paths of harmonic currents for the proposed universal control scheme.

D. Active Damping on CCTS

As shown in Fig. 2, the dynamics of the equivalent plant can be enhanced by the active damping method as [13] follows:

$$G'_p = \frac{G_P}{1 + K_d G_P} = \frac{1}{(R + K_d) + Ls} \tag{11}$$

where the K_d is the coefficient of active damping. It should be noted that the dynamics of disturbance rejection is determined by the slower one between the closed-loop bandwidth (α) and the plant dynamics [14]. The time constant of plant is usually longer than that of the closed-loop bandwidth. In order to obtain the identical dynamics of the closed-loop bandwidth, the coefficient of active damping can be designed as follows:

$$K_d = L\alpha - R. \tag{12}$$

$$\begin{aligned} \boldsymbol{I}_{dq} &= 0.5[\underbrace{I_{p1} e^{j\theta_{p1}} + I_{n2} e^{j(-2\omega_e t - \theta_{n2} + \pi)}}_{\text{First set of three - phase windings}} + \underbrace{I_{p2} e^{j\theta_{p2}} + I_{n2} e^{j(-2\omega_e t - \theta_{n2})}}_{\text{Second set of three - phase windings}}] \\ &= \underbrace{0.5\left(I_{p1} e^{j\theta_{p1}} + I_{p2} e^{j\theta_{p2}}\right)}_{\text{DC}}. \end{aligned} \tag{9}$$

E. Optimized Setting of Harmonic Current

The copper loss of dual three-phase PMSM can be expressed as follows:

$$P_{\text{cu}} = \frac{R_s}{T}\int_{t}^{t+T}\left[i_{dq}^2(t)+i_{z1z2}^2(t)\right] = \frac{R_s}{T}\int_{t}^{t+T}\left(\|\boldsymbol{I}_{dq}\|^2+\|\boldsymbol{I}_{z1z2}\|^2\right) \tag{13}$$

where $\|\ \|$ is the magnitude of the vector.

It is obvious from (13) that the optimized goal of harmonic-current reference is zero for normal operation. However, this traditional current setting may not be suitable for the fault-tolerant condition with the goal of minimum copper loss.

Substituting (9) and (10) into (13), according to Paswal's theorem, the copper loss can be calculated by the quadratic sum of magnitudes of different frequencies as follows:

$$P_{\text{cu}} = R_s\left(\|\boldsymbol{I}_{dq}\|^2+\left\|\boldsymbol{I}_{z1z2}^P\right\|^2+\left\|\boldsymbol{I}_{z1z2}^N\right\|^2\right). \tag{14}$$

As shown in (13) and (14), the minimum copper loss is related to the amplitudes of positive-sequence components, i.e., $\boldsymbol{I}_{z1z2}^P$ and the negative-sequence components, i.e., $\boldsymbol{I}_{z1z2}^N$ components of harmonic current. In order to solve the optimization problem, the relationship between the harmonic-current components and torque-current components will be discussed next.

From another perspective of the double *dq* model, the arbitrary setting of dc components of harmonic current in VSD also means that the amplitude ratio and phase shift of the positive-sequence components between two sets of three-phase windings can be arbitrarily adjusted as follows:

$$\boldsymbol{I}_{d1q1} = kIe^{j(\theta+\theta_{\text{shift}})},\quad \boldsymbol{I}_{d2q2} = Ie^{j\theta} \tag{15}$$

where k and θ_{shift} are the amplitude ratio and the phase shift of current vector between two sets of three-phase windings. I is the current amplitude of the second set of windings.

With the substitution of (15), the torque current in (9) can be rewritten as follows:

$$\boldsymbol{I}_{dq} = 0.5\left(kIe^{j(\theta+\theta_{\text{shift}})}+Ie^{j\theta}\right) = 0.5Ie^{j\theta}\left(1+ke^{j\theta_{\text{shift}}}\right). \tag{16}$$

Similarly, substituting (15) into (10), the dc terms of harmonic current in (10), i.e., the positive-sequence components in harmonic subspace, can be rewritten as follows:

$$\boldsymbol{I}_{z1z2}^P = 0.5\left(kIe^{j(\theta+\theta_{\text{shift}})}-Ie^{j\theta}\right)^* = 0.5Ie^{-j\theta}\left(ke^{-j\theta_{\text{shift}}}-1\right). \tag{17}$$

Comparing (16) and (17), the relationship between the torque-current components and the positive-sequence harmonic-current components can be illustrated as follows:

$$\boldsymbol{I}_{z1z2}^P = \left(ke^{-j\theta_{\text{shift}}}-1\right)/\left(1+ke^{-j\theta_{\text{shift}}}\right)\boldsymbol{I}_{dq}^*. \tag{18}$$

Splitting (18) into the real and imagery parts, the current reference in harmonic subspace can be derived from the amplitude ratio and phase shift as follows (19) shown at the bottom of this page.

It should be noted that the amplitude of negative-sequence current vector is same as that of the positive-sequence current vector under one-phase open-circuit faults. Hence, the amplitude of the negative-sequence current vector can also be derived from (16) as follows:

$$\left\|\boldsymbol{I}_{z1z2}^N\right\|^2 = \|I_{p2}\|^2 = \|\boldsymbol{I}_{d2q2}\|^2 = \left\|2\boldsymbol{I}_{dq}/\left(1+ke^{j\theta_{\text{shift}}}\right)\right\|^2. \tag{20}$$

Substituting (18) and (20) into (14), the copper loss of dual three-phase PMSM drives under one-phase open-circuit faults can be rewritten as follows:

$$P_{\text{cu}} = R_s\|\boldsymbol{I}_{dq}\|^2\left(1+\left\|\frac{ke^{-j\theta_{\text{shift}}}-1}{1+ke^{-j\theta_{\text{shift}}}}\right\|^2+\left\|\frac{2}{(1+ke^{j\theta_{\text{shift}}})}\right\|^2\right). \tag{21}$$

Normalized with respect to the copper loss ($P_{\text{base}} = R_s\|\boldsymbol{I}_{dq}\|^2$) under normal operation, the copper loss in (21) can be derived in per unit as given by

$$P_{\text{cu\_}n} = 1+\frac{(k\cos\theta_{\text{shift}}-1)^2+(k\sin\theta_{\text{shift}})^2+4}{(1+k\cos\theta_{\text{shift}})^2+(k\sin\theta_{\text{shift}})^2} = 1+\left(k^2-2k\cos\theta_{\text{shift}}+5\right)/\left(k^2+2k\cos\theta_{\text{shift}}+1\right). \tag{22}$$

Through the solution of extreme value solution for the multivariate function, it can be found that the minimum value of (22) can be reached with the amplitude ratio k of 3 and the phase shift θ_{shift} of zero as expressed by

$$\min P_{\text{cu\_}n} = P_{\text{cu\_}n}\left(k=3,\theta_{\text{shift}}=0\right) = 1.5. \tag{23}$$

It should be mentioned that the conclusion of (23) is based on the assumption that the open-circuit faults occurred in the second set of three-phase windings. For the fault position with the first set of three-phase windings, the conclusion of minimum copper loss can be updated as follows:

$$\min P_{\text{cu\_}n} = P_{\text{cu\_}n}\left(k=1/3,\theta_{\text{shift}}=0\right) = 1.5. \tag{24}$$

III. Experimental Verification

To verify the effectiveness of the proposed method, some experiments have been conducted on a laboratory prototype of dual three-phase PMSM drive fed by the two-level voltage-source inverter (VSI), which is composed of two sets of three-phase VSI sharing with the common dc bus. The detailed parameters of dual three-phase PMSM are listed in Table I, and the photograph for experimental setup of interior PMSM (IPMSM) platform is shown in Fig. 3. A digital signal processor of Texas Instrument TMS320F28335 has been used for the control algorithm,

$$I_{z1}^{\text{ref}} = \left[\left(k^2-1\right)\cdot I_d^{\text{ref}}-2k\sin\theta_{\text{shift}}\cdot I_q^{\text{ref}}\right]/\left(1+k^2+2k\cos\theta_{\text{shift}}\right)$$
$$I_{z2}^{\text{ref}} = \left[-2k\sin\theta_{\text{shift}}\cdot I_d^{\text{ref}}-\left(k^2-1\right)\cdot I_q^{\text{ref}}\right]/\left(1+k^2+2k\cos\theta_{\text{shift}}\right). \tag{19}$$

TABLE I
SYSTEM CONFIGURATION

Parameter	Value	Parameter	Value
Pole pairs	4	Stator resistance (R_s)	0.4 Ω
Rated speed	750 rpm	d-axis inductance (L_d)	10 mH
Rated torque	9.6 Nm	q-axis inductance (L_q)	12 mH
Rated current	10 A	Leakage inductance (L_σ)	5 mH
Maximum current	20 A	PM flux linkage (ψ_m)	0.09 Wb

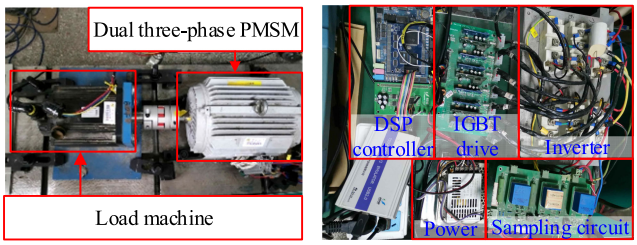

Fig. 3. Experimental setup. (a) Electrical machine. (b) Power circuits.

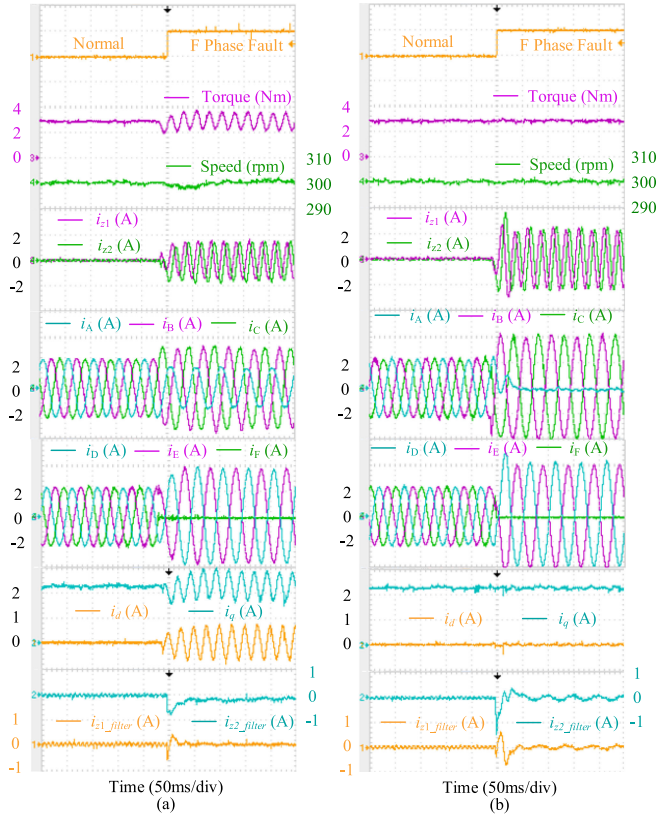

Fig. 4. Experimental results of different methods for dual three-phase IPMSM drive with phase F open-circuit faults (2.8 N·m @ 300 r/min). (a) Standard control method without fault tolerant. (b) Proposed universal control method.

where the switch frequency of power device and the sampling frequency are set to be 5 kHz.

Fig. 4 presents the experimental results of the standard pre-fault method and the proposed universal control method for phase F open-circuit faults. The standard prefault control method means the common control structure designed for the healthy

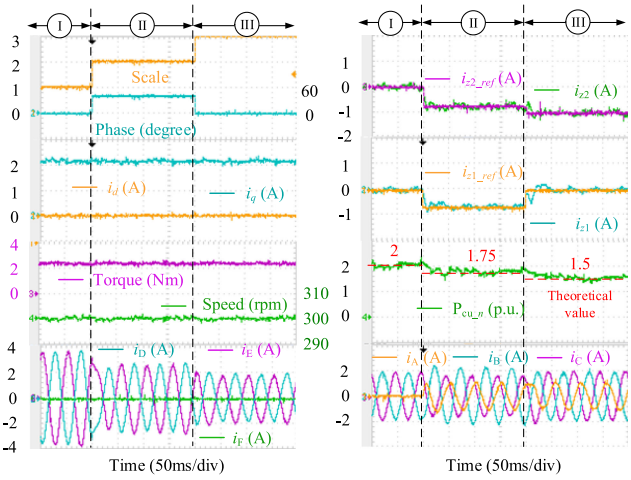

Fig. 5. Optimization setting of harmonic current for dual three-phase IPMSM drive with phase F open-circuit faults using the proposed methods: Case I: $k = 1$ and $\theta_{\text{shift}} = 0$; Case II: $k = 2$ and $\theta_{\text{shift}} = 42.10°$; and Case III: $k = 3$ and $\theta_{\text{shift}} = 0$.

TABLE II
COPPER LOSS UNDER DIFFERENT SETTINGS OF HARMONIC CURRENT

Harmonic current setting	Theoretical value (p.u.)	Experimental value (p.u.)
Case I: k=1 and θ_{shift}=0	2	[2, 2,2]
Case II: k=2 and θ_{shift}=42.10°	1.75	[1.7,1.8]
Case III: k=3 and θ_{shift}=0	1.5	[1.5,1.6]

situation in most existing pieces of literature, which usually include the CCTS and CCHS. The motor operates with a load torque of 2.8 N·m at 300 r/min. Owing to the absence of special fault-tolerant operation, the ripples in double of the fundamental frequency appear in the waveforms of the dq-axis current in torque subspace, which, in turn, leads to the torque ripples, as shown in Fig. 4(a). Meanwhile, the $z1z2$-axis current in harmonic subspace contains the ac components, which is out of control by setting the reference value to be zero. This phenomenon of torque ripples is consistent with the aforementioned theoretical analysis that CCHS and CCTS seem to seek the conflict goal owing to the negative-sequence components caused by the open-circuit faults.

When the $z1z2$-axis currents obtained from the notch filter are used for the control of harmonic current, almost no fluctuation appears in the waveforms of dq-axis current and torque with the proposed universal control method in Fig. 4(b). It should be pointed out that no diagnosis information is required for the proposed method and the same control configuration is adopted for the normal operation and fault-tolerant condition.

To verify the effectiveness of the proposed methods, different settings of harmonic current have been carried out for dual three-phase IPMSM drive with phase F open-circuit faults, as shown in Fig. 5. In spite of the variations of the amplitude ratio and the phase shift, the torque and dq-axis currents do not contain any ripples under the three cases. As can be seen from Table II, neglecting these fluctuations by the harmonic current, the final experimental results of normalized copper loss are coincided with the theoretical results. In a summary, the

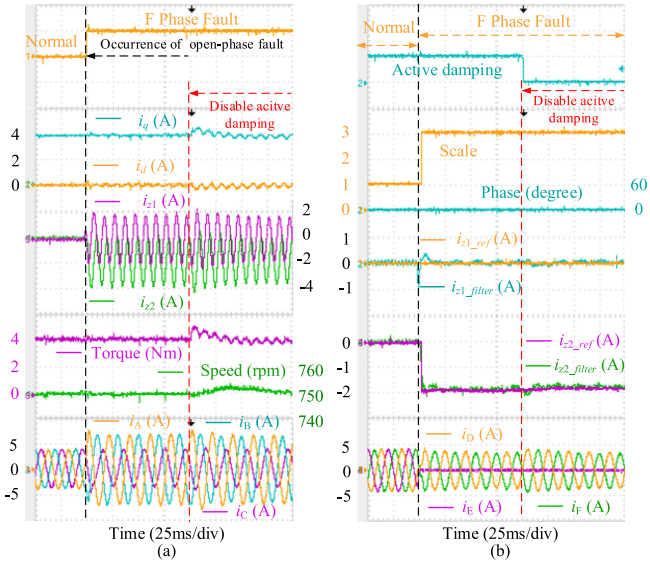

Fig. 6. Experimental results about active damping of the proposed universal control methods with open-circuit faults in phase E under the optimization of copper loss (4.3 N·m @ 750 r/min). (a) Torque current. (b) Harmonic current.

proposed optimization setting of harmonic current can achieve the minimum copper loss under the fault-tolerant condition.

Fig. 6 presents the experimental results of the proposed universal control methods with open-circuit faults in phase E at the rated speed of 750 r/min. The load torque is set as 4.3 N·m considering the power derating of postfault situation. From the waveforms of dq-axis currents and torque in Fig. 6, it can be observed that the proposed universal method realizes the seamless transition with torque-ripple-free performance between the normal operation and the fault-tolerant operation. In addition, the minimum copper loss can be achieved by adjusting the harmonic-current reference ($k = 3$ and $\theta_{\text{shift}} = 0$) after the fault localization. On the other hand, after the active damping is disabled, there appears the small ripples in torque due to the degrading disturbance rejection of CCTS. It can be concluded that the proposed universal control scheme with active damping can realize the natural fault tolerance of torque-ripple-free performance under rated condition.

IV. Conclusion

In this letter, a universal control scheme has been proposed for the normal operation and the fault operation of dual three-phase PMSM drives with two isolated neutral points. It is revealed that the presence of negative-sequence components of the faulty three-phase winding leads to incompatible control goal between CCHS and CCTS. In the proposed method, the notch filters have been inserted in the feedback of harmonic currents for the natural transition between healthy condition and faulty condition without the help of fault diagnosis. In addition, the minimum copper loss under postfault condition has been integrated into the proposed method by adjusting the positive-sequence components between two sets of three-phase windings. The comprehensive experiments have verified the effectiveness of the proposed method.

References

[1] E. Levi, F. Barrero, and M. J. Duran, "Multiphase machines and drives—Revisited," *IEEE Trans. Ind. Electron.*, vol. 63, no. 1, pp. 429–432, Jan. 2016.

[2] V. Yaramasu, A. Dekka, M. J. Duran, S. Kouro, and B. Wu, "PMSG-based wind energy conversion systems: Survey on power converters and controls," *IET Electr. Power Appl.*, vol. 11, no. 6, pp. 956–968, 2017.

[3] X. Wang, Z. Wang, Z. Xu, J. He, and W. Zhao, "Diagnosis and tolerance of common electrical faults in T-type three-level inverters fed dual three-phase PMSM drives," *IEEE Trans. Power Electron.*, vol. 35, no. 2, pp. 1753–1769, Feb. 2020.

[4] Z. Gao, C. Cecati, and S. X. Ding, "A survey of fault diagnosis and fault-tolerant techniques—Part I: Fault diagnosis with model-based and signal-based approaches," *IEEE Trans. Ind. Electron.*, vol. 62, no. 6, pp. 3757–3767, Jun. 2015.

[5] Z. Wang, Y. Wang, J. Chen, and M. Cheng, "Fault-tolerant control of NPC three-level inverters-fed double-stator-winding PMSM drives based on vector space decomposition," *IEEE Trans. Ind. Electron.*, vol. 64, no. 11, pp. 8446–8458, Nov. 2017.

[6] F. Baneira, J. Doval-Gandoy, A. G. Yepes, Ó. López, and D. Pérez-Estévez, "Control strategy for multiphase drives with minimum losses in the full torque operation range under single open-phase fault," *IEEE Trans. Power Electron.*, vol. 32, no. 8, pp. 6275–6285, Aug. 2017.

[7] H. Guzman et al., "Comparative study of predictive and resonant controllers in fault-tolerant five-phase induction motor drives," *IEEE Trans. Ind. Electron.*, vol. 63, no. 1, pp. 606–617, Jan. 2016.

[8] Z. Wang, X. Wang, J. Cao, M. Cheng, and Y. Hu, "Direct torque control of T-NPC inverters-fed double-stator-winding PMSM drives with SVM," *IEEE Trans. Power Electron.*, vol. 33, no. 2, pp. 1541–1553, Feb. 2018.

[9] I. G. Prieto, M. J. Duran, P. Garcia-Entrambasaguas, and M. Bermudez, "Field-oriented control of multiphase drives with passive fault tolerance," *IEEE Trans. Ind. Electron.*, vol. 67, no. 9, pp. 7228–7238, Sep. 2020.

[10] X. Wang, Z. Wang, M. Gu, D. Xiao, J. He, and A. Emadi, "Diagnosis-free self-healing scheme for open-circuit faults in dual three-phase PMSM drives," *IEEE Trans. Power Electron.*, vol. 35, no. 11, pp. 12053–12071, Nov. 2020.

[11] K. Yu, Z. Wang, X. Wang, and Z. Zou, "An online flux estimation for dual three-phase SPMSM drives using position-offset injection," *IEEE Trans. Power Electron.*, vol. 36, no. 10, pp. 11606–11617, Oct. 2021.

[12] C. L. Fortescue, "Method of symmetrical co-ordinates applied to the solution of polyphase networks," *Trans. Amer. Inst. Elect. Engineers*, vol. 37, no. 2, pp. 1027–1140, Jul. 1918.

[13] F. B. del Blanco, M. W. Degner, and R. D. Lorenz, "Dynamic analysis of current regulators for AC motors using complex vectors," *IEEE Trans. Ind. Appl.*, vol. 35, no. 6, pp. 1424–1432, Nov./Dec. 1999.

[14] R. Ottersten, "On control of back-to-back converters and sensorless induction machine drives," Ph.D. dissertation, Dept. Electr. Power Eng., Chalmers Univ. Technol., Gothenburg, Sweden, 2003.